Multiple Weather Regimes and Baroclinically Forced Spherical Resonance

SHUTING YANG,* BRIAN REINHOLD, AND ERLAND KÄLLÉN

Department of Meteorology, University of Stockholm, Stockholm, Sweden

(Manuscript received 18 May 1995, in final form 19 January 1996)

ABSTRACT

Systematically recurrent, geographically fixed weather regimes forced by a single isolated mountain in a two-layer, high-resolution, quasigeostrophic model modified for the sphere are found to be robust phenomena. While the climatological stationary wave is often confined to (or has maximum amplitude in) the region just downstream of the orography, giving the appearance of a wave train propagating into the Tropics, the regional maximum centers of low-frequency variance appear around the hemisphere, giving the appearance of zonal resonance or some type of zonally confined propagation. This result is not anticipated in light of Rossby wave dispersion theory on the sphere. On the other hand, baroclinic disturbances developing on a meridional temperature gradient of finite extent force subtropical and polar easterlies as well as a sharpened midlatitude westerly jet, which provides a zonal waveguide (by refraction and/or reflection) for the Rossby waves. These conditions are favorable for the establishment of multiple weather regimes. The baroclinicity of the atmosphere is then continuously forcing a mean state that favors forced zonal propagation, counteracting the meridional dispersion generated by the spherical geometry alone. These ideas suggest that the multiple-equilibria theories may be more applicable to the atmosphere than originally suggested by linear dispersion theory on the sphere. It may also help explain why channel models work as well as they do even for the largest scales.

1. Introduction

Observations of the large-scale flow in the Northern Hemisphere by several authors using a variety of techniques [point correlations and teleconnections, Wallace and Gutzler (1981); point selection and persistent anomalies (Dole and Gordon 1983; Dole 1986); cluster analysis, (Mo and Ghil 1988); etc.] reveal the presence of multiple, systematically recurring, persistent states that appear to have rapid onsets and breakdowns (Dole 1986; Yang and Reinhold 1991). General circulation model (GCM) experiments further demonstrate that these patterns can develop, persist, and decay without any time variations in the boundary conditions (Lau 1981; Blackmon et al. 1986), suggesting that the fundamental dynamics of these phenomena is internal.

The pioneering work of Charney and DeVore (1979), hereafter CDV, offers a new hypothesis to account for these phenomena. In a low-order, beta-plane, barotropic channel model forced by a periodic sinusoidal orography, CDV find two stable flow states. These multiple flow equilibria are proposed to form the attractors for the observed quasi-persistent states of the atmosphere. The existence of stationary multiple flow equilibria is confirmed by several following studies in slightly more sophisticated, baroclinic large-scale channel models (Charney and Straus 1980; Roads 1980a,b; Pedlosky 1981) and a low-order spherical model with parameterized transient eddy forcing (Källén 1981). The concept is extended by Reinhold and Pierrehumbert (1982), hereafter RP, to include the synoptic-scale baroclinic waves in the balances. The spatial organization of the baroclinic eddies by the large-scale flow leads to an internal feedback upon the large-scale flow that can come to multiple, quasi-equilibrated states. This dynamical balance is referred to as a weather regime, and it is shown to explain the quasi-persistent states observed in the low-order baroclinic channel model of RP and Vautard and Legras (1988) further demonstrate that the regime-equilibrium balance of RP is able to explain the multiple persistent flow states in a much higher resolution version of a channel model with a localized thermal forcing instead of orography as the source of zonal inhomogeneity.

However, in all the aforementioned studies, either the channel model geometry or a high level of truncation leads to an artificial forced zonal propagation that constrains the disturbances to propagate along latitude circles. Without this forced zonal propagation, the possibility of barotropic resonance becomes questionable. Since resonance and resonance bending are essential elements of the multiple flow equilibria of CDV, these

* Current affiliation: Danish Meteorological Institute, Copenhagen, Denmark.

Corresponding author address: Dr. Brian Reinhold, Department of Meteorology, University of Stockholm, S-106 91 Stockholm, Sweden. E-mail: brian@misu.su.se

equilibria may be difficult to obtain in high-resolution systems on the sphere, where there is no a priori meridional confinement of the disturbances (Held 1983; Källén 1985).

Theoretical grounds for this insight are based upon the analysis of Rossby wave dispersion in a background potential vorticity gradient, in particular the meridional gradient of the beta effect present on the sphere (Hoskins and Karoly 1981). The variable beta implies that the local meridional wavenumber of the stationary Rossby wave changes with latitude, locally altering the shape, amplitude, and group velocity. Thus the disturbance propagates in wave trains along great circle arcs. Thus disturbances generated by an isolated source of midlatitude forcing could propagate out of the midlatitudes, eliminating the potential for resonance. Such wave train behavior is clearly demonstrated in spherical barotropic and baroclinic models linearized about slowly varying zonal flows (Grose and Hoskins 1979; Hoskins and Karoly 1981; Held 1983).

On the other hand, there are two features that may limit the degree to which large-scale disturbances propagate out of the midlatitudes. The first is that the curvature of the jet can be a significant part of the background potential vorticity gradient and may more than compensate for the meridional variation of the beta effect. The second is that linear theory breaks down in the vicinity of a zero wind line (Held 1983). Thus resonant-like behavior may still be possible depending on whether the curvature of the jet and/or the dynamics in the vicinity of the zero wind line provide significant refraction and/or reflection of the incident waves. Indications of forced zonal propagation, or waveguide-type behavior, are seen by Branstator (1983), who finds that stationary waves appear to propagate along a strong jet in an idealized slowly varying flow. A more comprehensive theoretical analysis of these situations is provided by Hoskins and Ambrizzi (1993). They show that if the basic state possesses a local maximum in the stationary Rossby wavenumber, the basic-state flow will act as a waveguide. This condition is most likely to occur in a strong westerly jet; thus Rossby wave energy excited by isolated orography may be funneled along the jet axis and return to the source region, setting the stage for resonance.

The purpose of this study is to investigate why the baroclinic weather regime phenomenon is so robust on the sphere in spite of the fact that the forced zonal propagation present in the channel models used by RP and Vautard and Legras (1988) does not exist. Robust regimes have also been noted in simpler spherical models, such as the three-level quasigeostrophic spherical model of Marshall and Molteni (1993), which has, in addition to orography, a relaxation to an atmospheric-like climatological streamfunction. We hypothesize that one possible explanation for the ubiquitous regime or persistent anomaly behavior in these models is that, since the equilibrated baroclinic disturbances systematically generate a mean field with a sharp westerly jet and easterlies at the periphery, the shape of the climatological flow always tends to mitigate the meridional dispersion caused by the sphericity. The result is that the zonal propagation is enhanced over that which would be anticipated based upon linear considerations.

To examine this hypothesis with a model that is physically as close as possible to the quasigeostrophic models used by the majority of multiple flow equilibria and weather regime studies, the quasigeostrophic, two-layer model of the aforementioned studies are appropriately modified for the sphere (Lorenz 1960). This system includes the full variation of the Coriolis parameter. However, even spherical models will impose an a priori forced zonal propagation if they are too severely horizontally truncated, especially meridionally. A resolution of T21 seems to be sufficient to allow meridional propagation.

In the following sections, we start with a description of the model and the primary physical differences between the spherical and beta-plane baroclinic, quasigeostrophic equations. The weather regime behavior (as measured by frequencies of persistent anomalies) in general produced by this model is then presented, with the major focus on the ubiquitous occurrence of weather regimes that appear for a wide range of the parameters as long as there is some source of zonally inhomogeneous forcing. Two cases are then selected in which the structure of the baroclinically forced time mean flows gives an excellent versus poor waveguide. The phenomenon of ''resonance'' or zonal propagation is examined in these two extreme cases. We then discuss other possible mechanisms besides the formation of waveguides by the equilibrated baroclinic eddies that may account for the robust occurrence of weather regimes in a baroclinic atmosphere on a sphere.

2. The model

We use a two-layer, quasigeostrophic model originally derived by Lorenz (1960), which is formulated as follows:

$$\frac{\partial}{\partial t}\nabla^2\psi = -\mathrm{J}(\psi, \nabla^2\psi + f + f_0\hbar/H) - \mathrm{J}(\tau, \nabla^2\tau - f_0\hbar/H) - \frac{1}{2}\varepsilon_d\nabla^2(\psi - \tau), \quad (1)$$

$$\frac{\partial}{\partial t}\nabla^2\tau = -\mathrm{J}(\psi, \nabla^2\tau - f_0\hbar/H) - \mathrm{J}(\tau, \nabla^2\psi + f + f_0\hbar/H) + \boldsymbol{\nabla}(f\boldsymbol{\nabla}\chi) + \frac{1}{2}\varepsilon_d\nabla^2(\psi - \tau) - 2\varepsilon_i\nabla^2\tau, \quad (2)$$

$$\frac{\partial}{\partial t}\theta = -\mathrm{J}(\psi, \theta) + \sigma\nabla^2\chi + \delta(\theta^* - \theta), \quad (3)$$

$$b_0c_p\nabla^2\theta = \boldsymbol{\nabla}(f\boldsymbol{\nabla}\tau), \quad (4)$$

where $\psi = (\frac{1}{2})(\psi_1 + \psi_3)$, $\tau = (\frac{1}{2})(\psi_1 - \psi_3)$, and $\theta = (\frac{1}{2})(\theta_1 + \theta_3)$ define the barotropic and baroclinic parts of the streamfunction and the vertically averaged perturbation potential temperature, respectively, and the subscripts 1 and 3 refer to the middle of the upper and lower layers. The static stability σ is the difference between the horizontally averaged potential temperature in each layer and is assumed to be constant. The velocity potential at the lower layer is given by $\chi = \chi_3 = -\chi_1$, and f is the latitudinally varying Coriolis parameter $2\Omega \sin\phi$, where Ω is the angular velocity of the earth and ϕ is latitude. Damping parameters are ε_d and ε_i, which are the Ekman damping coefficients at the surface and between the layers, respectively, and δ is the Newtonian cooling coefficient. The model is forced by a prescribed radiative relaxation temperature field, θ^*, and topography. The topographic forcing has been parameterized by $J(\psi, f_0 h/H)$, where $f_0 = 2\Omega$ is a constant, H is the thickness of each layer, and h is the dimensional topographic height. On the sphere, the correct expression for the topographic forcing is given by $J(\psi, fh/H)$, which can be derived from the equation for the conservation of barotropic potential vorticity (Marshall and Molteni 1993). However, as long as the orography is confined to the extratropics, the numerical simplification of a constant Coriolis parameter has minor influences, an assumption supported by the results of Hendon (1986), which we discuss later. The principal alteration is that the effective height of the mountain is greater toward the equator than implicated by h alone. However, this simplification does not influence the study concerning meridional Rossby wave dispersion as we only consider nonzero orographic forcing north of 30°N. The remaining constant b_0 is defined as $b_0 = \frac{1}{2}[(p_3/p_{00})^\kappa - (p_1/p_{00})^\kappa]$, where p_1 and p_3 are the pressure levels at the center of the two layers (250 hPa and 750 hPa, respectively), p_{00} is the surface pressure (1000 hPa), and $\kappa = R/c_p = 2/7$, where R is the gas constant and c_p the specific heat of air at constant pressure. The Jacobian $J(A,B)$ and the Laplace operator ∇^2 are defined by

$$J(A, B) = a_0^{-2}\left[\frac{\partial A}{\partial \lambda}\frac{\partial B}{\partial \mu} - \frac{\partial A}{\partial \mu}\frac{\partial B}{\partial \lambda}\right]$$

$$\nabla^2 = a_0^{-2}\left\{\frac{\partial^2}{\cos\phi \partial \lambda^2} + \frac{\partial}{\partial \mu}\left[\cos^2\phi \frac{\partial}{\partial \mu}\right]\right\},$$

where a_0 is the radius of the earth, λ is longitude, and $\mu = \sin\phi$.

The system given by Eqs. (1)–(4), which Mak (1991) refers to as a linear balance model, differs from a conventional quasigeostrophic beta-plane model in the sense that it includes the full variation of the Coriolis parameter. The variable Coriolis parameter leads to a more complicated expression for the baroclinic feedback in the model, so that the τ equation becomes implicit. The model, on the other hand, is integrable and balanced on the entire sphere including the equator for any arbitrary initial conditions of ψ and τ.

The dependent variables ψ and τ are expanded into a series of spherical harmonies truncated at triangular wavenumber 42 and/or 21, which is judged to be of sufficiently high resolution that both local orography and meridional dispersion are adequately described. A detailed description of the spectral form of the model in the spherical domain is given in the appendix.

The model is driven by a thermal radiative relaxation forcing, θ^*, which is zonally homogeneous. Other model parameters include the Ekman damping and Newtonian cooling coefficients ε_d, ε_i, and δ, which are also zonally homogeneous. The only zonal inhomogeneity in the model is provided by orography consisting of either one or two isolated mountains in the Northern Hemisphere. A single isolated mountain is formulated as

$$h = h_0 \sin\{(\lambda - \lambda_0)\pi/\Delta\lambda\}\sin\{(\phi - \phi_0)\pi/\Delta\phi\},$$

$$\text{for } |\lambda - \lambda_0| < \Delta\lambda \text{ and } |\phi - \phi_0| < \Delta\phi;$$

$$h = 0 \quad \text{outside this region,}$$

where h_0, λ_0, and ϕ_0 are the maximum height, the westmost longitude, and the southmost latitude of the mountain, respectively, and F_λ and F_ϕ are the longitudinal and meridional widths. The mountain is placed at northern midlatitudes with a height of $h_0/H = 0.4$ in all experiments. A biharmonic diffusion ($\upsilon\nabla^6$) of vorticity is also included in the model with $\upsilon = 7.0 \times 10^{16}$ m^4 s^{-1}. Each experiment consists of a 2000-day integration from an initial state consisting of the zonally symmetric so-called Hadley solution of the model with a small perturbation arbitrarily inserted into some of the wave components such that all wave components are potentially generated. The model statistics are derived from samples taken twice daily, after an initial spinup period of 100 days that is discarded.

3. Model climatology and weather regimes

A series of experiments are performed with different parameter sets as well as different horizontal resolutions (T21 and T42 models). Though most runs use a thermal forcing symmetric about the equator, experiments are done with asymmetric forcing as present during solstice seasons. Experiments are also done with isolated mountain(s) of different width (and spacing). To examine if there are weather regimes, we adopt Dole's method (Dole and Gordon 1983) to look for persistent anomaly events. Following Dole and Gordon (1983), a ''persistent anomaly'' at a point is identified if an anomaly at that point exceeds some threshold magnitude value (M) for a specified duration (T) (see their Fig. 1 for reference). The method is then applied to the 500-hPa low-pass filtered streamfunction field for every grid point of the entire model domain, where the low-pass filter (Blackmon 1976) emphasizes fluctuations with periods

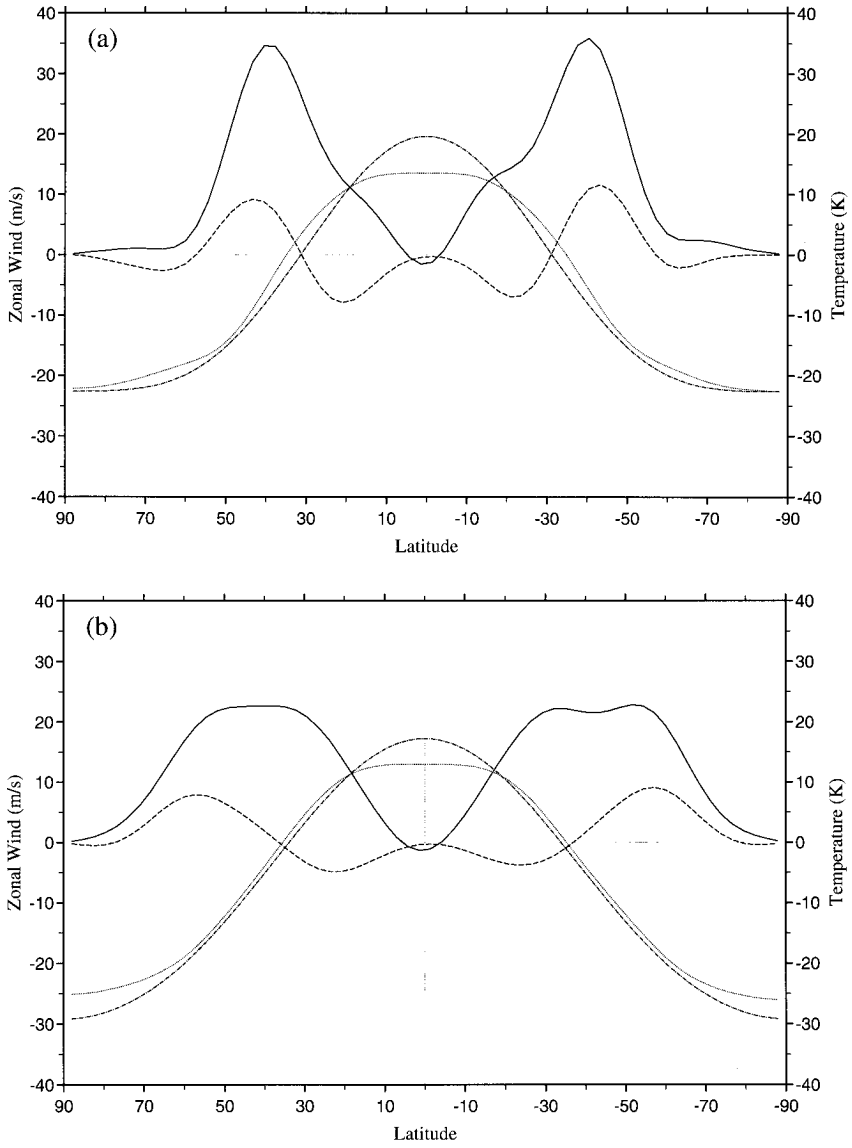

FIG. 1. The climatological zonal mean fields in (a) the steep jet case and (b) the flat jet case. The upper- and lower-level zonal winds are shown by the solid and dashed lines. The zonal mean temperatures at the middle level are shown by the dotted lines. The thermal forcing profiles in the two cases are given by the dash–dotted lines.

longer than 10 days. Though the choice of the criteria (M, T) is arbitrary, we hope that by applying this method we can identify persistent weather regimes that are distinct from the synoptic activity. For this purpose, we choose T to be 10 days and the magnitude of the anomaly M to be about 0.7 times the maximum root-mean-square streamfunction at 500 hPa. Other values are tested, and the results are similar to that of Dole and Gordon (1983), in that the number of events simply decreases with more stringent requirements, but the locations and polarities still prevail.

The common result in all of the mountain experiments that is important to the goals of this study is that there are always geographically fixed centers of low-frequency variability around the Northern Hemisphere. In addition, these maxima are coincident with the centers of the maximum in frequency of persistent anomalies as identified by Dole's criteria or weather regimes. In the Southern Hemisphere, all patterns are zonally symmetric as anticipated. However, in spite of the lack of any zonally inhomogeneous external forcing in the Southern Hemisphere, the amount of low-frequency variance is about equal to that in the Northern Hemisphere. On the other hand, the number of persistent anomaly events in the Southern Hemisphere is about an order of magnitude less.

These results have also been noted by Hendon (1986), with the exception of the persistent anomaly statistics, which were not computed in his locally orographically forced, two-layer, spherical primitive equation model. Hendon's (1986) primitive equation model is constructed such that there is no time or spatial variability of the static stability, which makes it dynamically similar to a quasigeostrophic model. Hendon does include a variable Coriolis parameter in his orographic forcing term, which further demonstrates that our approximation of a constant Coriolis parameter in the orographic forcing does not lead to any serious errors.

In general, our model overestimates the low-frequency variability relative to the bandpass or synoptic timescale activity (about 10 to 1 compared to 3 to 1 for the Northern Hemisphere) and underestimates the persistence of the weather regime states [as defined by Dole and Gordon's (1983) persistent anomalies] relative to the atmosphere. Even our cases with the highest number of persistent events did not have as many events as identified by Dole and Gordon for the atmosphere, and the probability that an event would persist one more day (given that it had persisted x days) is always less than Dole and Gordon's observations. The low-frequency behavior of this model is then much more smoothly varying than in the atmosphere.

The climatological stationary wave is only significant in the Northern Hemisphere. The wave pattern is always present as a ridge to the west of and a trough to the east of the orographic ridge. But thereafter, the intensity and the structure of the pattern is highly parameter dependent. Of course, subtle phase changes of the waves can easily eradicate any signal in the stationary waves, especially far from the mountain. Furthermore, asymmetries in the multiple-regime states also contribute to a weaker stationary wave signal. Consequently, it is difficult to draw any distinct conclusions about the hemispheric quasi-stationary large-scale behavior from these statistics.

The climatological zonal mean flow statistics for symmetric thermal forcing are only slightly influenced by orography, and thus appear quite symmetric about the equator. However, their meridional structure, which is determined primarily by baroclinic disturbances, is of particular importance as they form the waveguides that force zonal propagation. The surface flows always consist of subtropical easterlies, midlatitude westerlies, and often polar easterlies. The upper-level flows consist of strong midlatitude westerly jets (sometimes with a double jet signature) and often easterlies in the equatorial region.

This mean flow structure of a westerly jet bounded by surface subtropical and often polar easterlies is a fundamental feature of equilibrated baroclinic waves and it is equally prominent in the two-level channel (O'Brien and Branscome 1989) or multilevel channel as it is on the sphere. The exact causes of this profile are beyond the scope of this study, but qualitatively it can be seen that if the temperature gradient has a finite meridional extent, the fastest growing initial baroclinic disturbances that develop will have a meridional extent of the same order. The barotropic feedbacks forced by these structures tend to further meridionally confine the jet, but the barotropic nature of this process is less effective at confining the temperature gradient. Consequently, surface easterlies develop along the peripheries of a sharpened midlatitude westerly jet.

4. Steep jet versus flat jet case

To examine the above hypothesis concerning baroclinically generated waveguides and resonant-like behavior, we analyze a case in which the time mean zonal flows have well-defined maxima in the local stationary wavenumber against one in which the maxima are practically nonexistent. The first case will be referred to as the ''steep jet,'' while the second will be referred to as the ''flat jet'' case.

The only difference between these two cases is the shape of the radiative relaxation temperature profile (θ^*), which can be seen as thin solid lines in Figs. 1a,b. Both profiles consist of only the two largest symmetric modes $(m, n) = (0, 2)$ and $(0, 4)$, where m and n indicate zonal and total wavenumber. The coefficient of mode $(0, 2)$ is -14.4 K for both cases, while the $(0, 4)$ mode is 3.2 K and 1.0 K for the steep jet and flat jet case, respectively. The model is truncated at T21. Otherwise, the static stability (σ) is given by 17.3 K, and the damping decay rate at the surface (ε_d^{-1}) is 5 days, between the layers (ε_i^{-1}) is 20 days, and the Newtonian cooling rate (δ^{-1}) is 10 days. A mountain of longitudinal and latitudinal width of 45° is centered at 45°N as shown by the thin solid line in Fig. 3.

The differences in the forcing profiles shown in Figs. 1a,b are not too apparent by eye. However, the southward shift of the maximum temperature gradient in the steep jet case leads to a more equatorward and more meridionally confined jet, as can be seen by the solid lines (upper-level winds) and the dashed lines (lower-level winds) in Fig. 1.

Using Eqs. (2.12) and (2.13) of Hoskins and Ambrizzi (1993), we can estimate the degree to which the upper-level time mean zonal flows shown in Fig. 1 act as a potential waveguide. The results for the steep jet and flat jet case are shown in Figs. 2a and 2b, respectively. In both cases, a local maximum in the stationary Rossby wavenumber is observed at the midlatitudes, which, according to Hoskins and Ambrizzi (1993), is indicative of a waveguide, since Rossby wave energy refracts toward increasing wavenumber. However, the latitudinal width of the waveguide is much larger in the steep jet case, and thus the steep jet case should be more effective at forcing zonal propagation if the linear ideas hold for the full model.

Examination of the time-averaged waves of the two cases in Figs. 3a,b support this speculation. While the

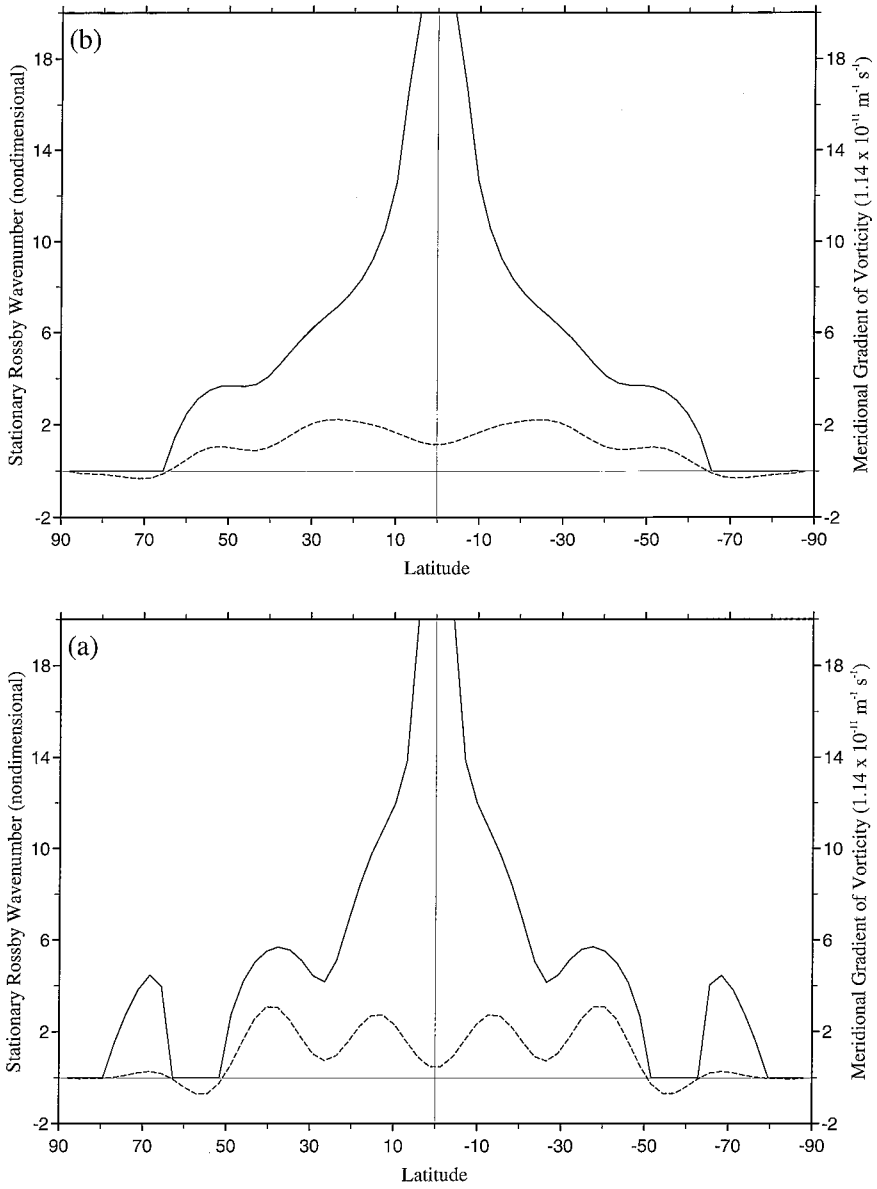

FIG. 2. The meridional gradient of the time mean absolute vorticity (dashed line, unit: 1.14×10^{-11} m^{-1} s^{-1}) and the corresponding stationary Rossby wavenumber calculated from the upper-level time mean zonal wind (solid line, nondimensional). The stationary wavenumber is defined only for positive zonal winds and positive absolute vorticity gradients (see Hoskins and Ambrizzi 1993 for definition and explanations). (a) The steep jet case. (b) The flat jet case.

flat jet case (Fig. 3b) shows a primarily regional wavetrain propagating into the subtropics, the steep jet case (Fig. 3a) shows a distinct, meridionally confined zonal wavenumber-5 pattern, though the amplitude of the waves successively diminishes downstream of the mountain.

A more quantitative measure of the waveguide can be obtained by computing the horizontal fluxes of the climatological stationary wave activity (Plumb 1985). To make this computation, the climatological waves at the upper level shown in Figs. 3a,b are utilized and the results are presented in Figs. 4a and 4b, respectively. As shown by Plumb (1985), the stationary wave activity flux is parallel to the group velocity, while the local divergence (convergence) of the fluxes indicates a source (sink) of the stationary waves. From the direction of the flux arrows in the steep jet case (Fig. 4a) we see clearly that the energy flow is refracted and/or reflected very strongly along the jet axis. In the flat jet case (Fig. 4b), on the other hand, most of the

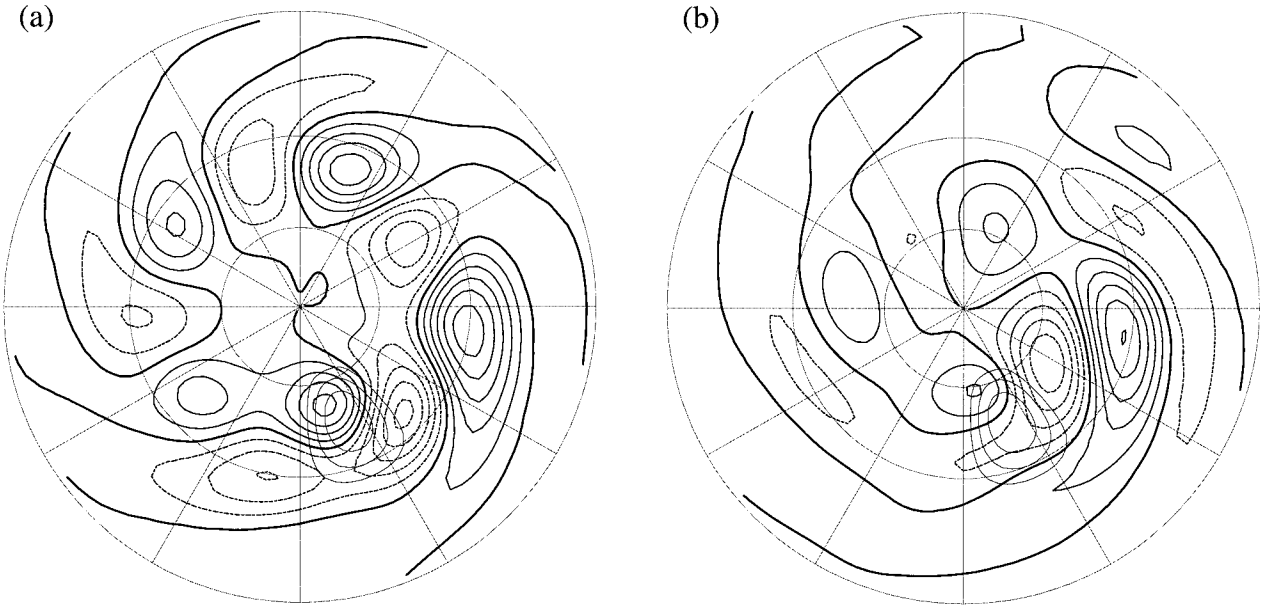

FIG. 3. Polar stereographic projection of the climatological stationary waves of the upper-level streamfunctions in (a) the steep jet case and (b) the flat jet case. Contour interval is 3.0×10^6 m^2 s^{-1}. Thinner contours indicate the height of the orography. The contour interval is $h_0/4$, where h_0 is the height of the mountain.

flux is directed into and absorbed at the subtropics, with only a weak indication of zonal funneling at about 60°N.

Since there are weather regimes in both of these cases, the stationary wave activity flux may vary substantially from those based upon the climatological stationary waves discussed here. Nevertheless, the persistent anomaly statistics for the steep jet and flat jet cases shown in Figs. 5a and 5b, respectively, suggest that the zonal waveguide properties have a strong influence on the regimes. In the steep jet case, the persistent anomaly centers possess an almost perfect zonal wavenumber-5 pattern with each center having a nearly equal frequency of occurrence, regardless of the downstream distance from the mountain. In contrast, the centers of the flat jet case, which are still present about

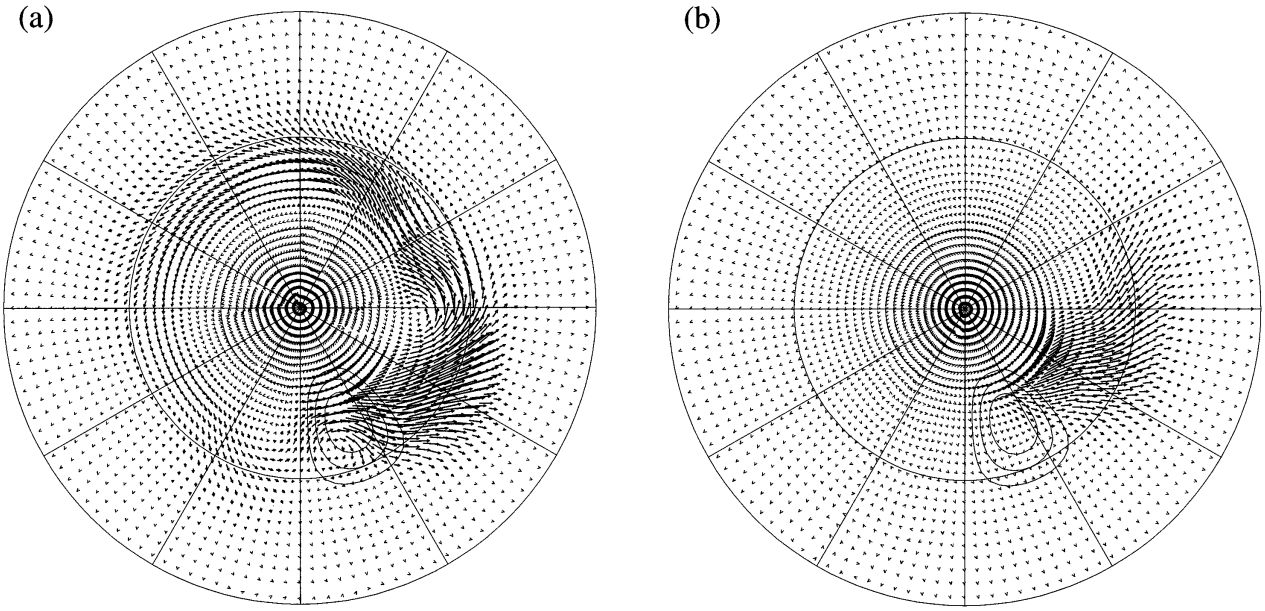

FIG. 4. The horizontal stationary wave activity flux computed from the climatological waves shown in Fig. 3. (a) The steep jet case. (b) The flat jet case. The maximum vector has a magnitude of 23.1 m^2 s^{-2} in (a) and 14.0 m^2 s^{-2} in (b).

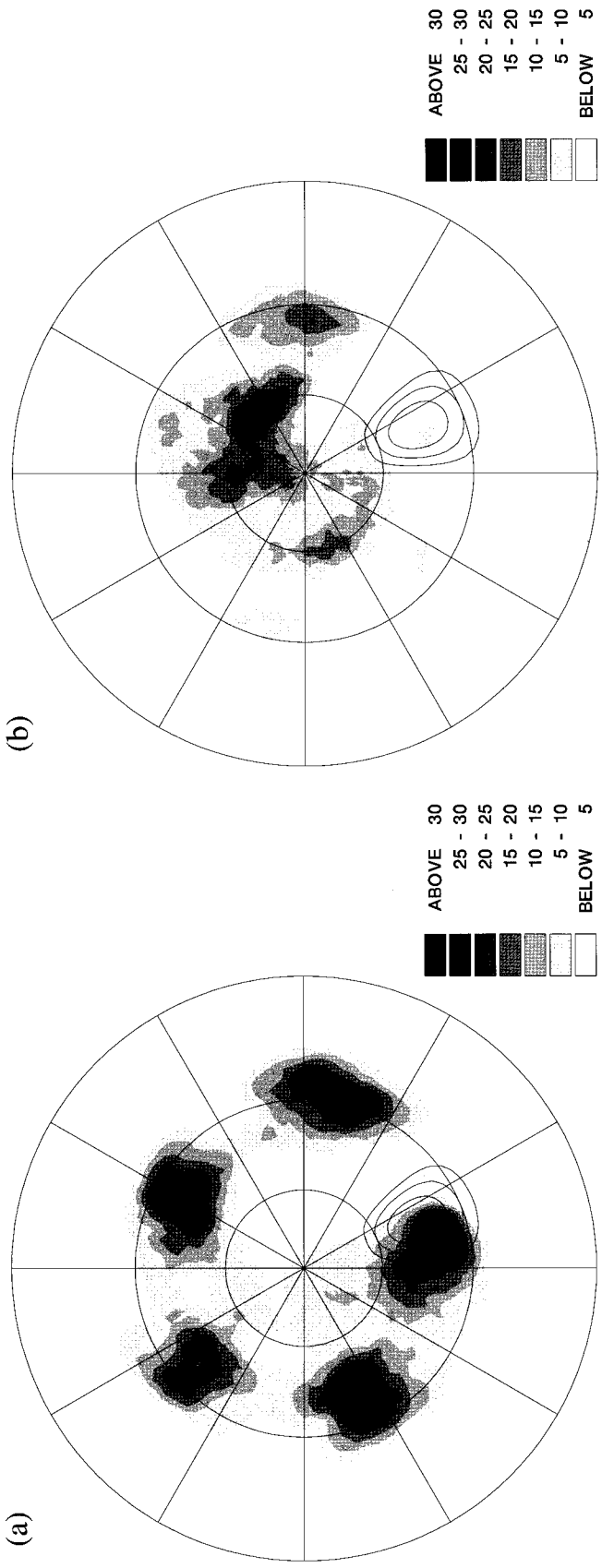

FIG. 5. The geographical distribution of the total number of positive and negative persistent anomaly events satisfying a duration criterion of 10 days and a magnitude criterion of 0.7 times the root-mean-square streamfunction. (a) The steep jet case and (b) the flat jet case.

the hemisphere, are much more disorganized. However, the maximum number of events is located at 60°N, downstream of the weak zonal transport along the waveguide shown in the stationary wave activity flux calculation, implying that the weak waveguide plays a role. The waveguide, on the other hand, seems so weak that the zonal propagation of stationary wave energy hardly completes one circle, suggesting that there may be other processes involved in the establishment of weather regimes in this case.

An important characteristic of resonance in general is that the response increases dramatically when the forcing is in phase with the resonant frequency or spatial scale. To demonstrate the resonant-like character of the steep jet case, we place a second mountain first in phase and then out of phase with the observed single-mountain response. As anticipated, the response, or the number of persistent anomaly events, increases for the in-phase forcing (Fig. 6a) and decreases for the out-of-phase forcing (Fig. 6b). This behavior clearly illustrates the resonant-like character of the response and the direct influence of the zonally inhomogeneous forcing of the mountain.

5. Discussion and conclusions

In this study we have shown that a two-layer, T21 resolution quasigeostrophic model on the sphere forced by isolated orography possesses multiple weather regimes and/or persistent anomalies and geographically fixed centers of low-frequency variance around the entire hemisphere. These results remain the case even when the climatological stationary wave only has significant amplitude in the vicinity of the orography. The hemispheric response is highly consistent with the results of channel models even though there is no analogous a priori elimination of meridional propagation. We hypothesize that these results are in part due to the meridional profile of the mean zonal flows forced by equilibrated baroclinic eddies. These eddies always act to generate subtropical surface easterlies and sharpened midlatitude westerly jets, which then act as waveguides and funnel the Rossby wave energy more or less along the jet axis. Calculations of the wave activity fluxes show signs of this funneling and thus support the hypothesis. Consequently, in spite of the spherical geometry, the baroclinic disturbances tend to drive a climatological mean flow that favors barotropic zonal propagation and thus the potential for resonance, similar to the channel model behavior. The even more robust regime behavior of the Marshall and Molteni (1993) three-layer quasigeostrophic model over our model may then be partly accounted for by their imposed relaxation to a climatological flow field.

The conditions for weather regimes in this spherical model are then similar to many of the channel model studies, and this is thus one reason why the spherical model is as effective at generating weather regimes as the channel models. It is, in fact, difficult in our model to find reasonable parameter sets where the baroclinic eddies do not establish a jet structure that does not strongly mitigate the meridional propagation of the variable Coriolis parameter. Since the time mean zonal winds of the atmosphere are also bounded by tropical easterlies with a midlatitude maximum in the westerlies, it is likely that the meridional propogation characteristics of the variable beta effect are similarily compromized.

On the other hand, since the waveguide on the sphere is not always constrained to exist as in the channel, the quality of the waveguide is both parameter dependent, as demonstrated by the two extreme cases, and time dependent. The degree of resonant-like behavior or zonal propagation is then much more free to vary. The quality and strength of the waveguide, as well as the details of how the refraction occurs, may be one mechanism leading to the type of regionality observed in atmospheric weather regime patterns (Reinhold 1987).

However, even the lack of a barotropic waveguide does not rule out the existence of resonant-like weather regimes in a baroclinic system, due to the role of organized baroclinic instabilities or storm tracks in the weather regime balances. Energy may be ''propagated'' by spatially modulated synoptic-scale baroclinic instability. The large-scale response downstream of the mountain, even if it propagates into the subtropics, can organize the instabilities farther downstream into storm tracks. These storm tracks will act as a source of zonally inhomogeneous forcing that generates further downstream large-scale disturbances, whereupon the process repeats. This refeeding of localized large-scale energy into the system by baroclinic instability may also be sufficient to produce an effective resonant type of response in the presence of large dissipation, although in a barotropic system large dissipation can eliminate the potential for resonance (Held 1983). The important role of the baroclinic transient eddies upon the large-scale, persistent anomalous flow has been suggested by Shutts (1983). He shows that traveling eddies steered by a large-scale diffluent flow transmit energy to the large-scale flow, which reinforces blocked flow patterns.

The main result of this study is that baroclinic waves tend to generate a meridional jet structure that favors the zonal propagation of orographically forced waves, or at least mitigates the meridional propagation characteristics induced by the variable Coriolis parameter on the sphere. This reduction of meridional propagation creates a possibility for hemispheric resonance or resonant-like behavior and we do indeed find the type of weather regime behavior that has been attributed to resonant behaviour in earlier studies. A spherical geometry therefore does not rule out resonant behavior as suggested by Held (1983) and Källén (1985). In this light, the multiple equilibrium theories as originally

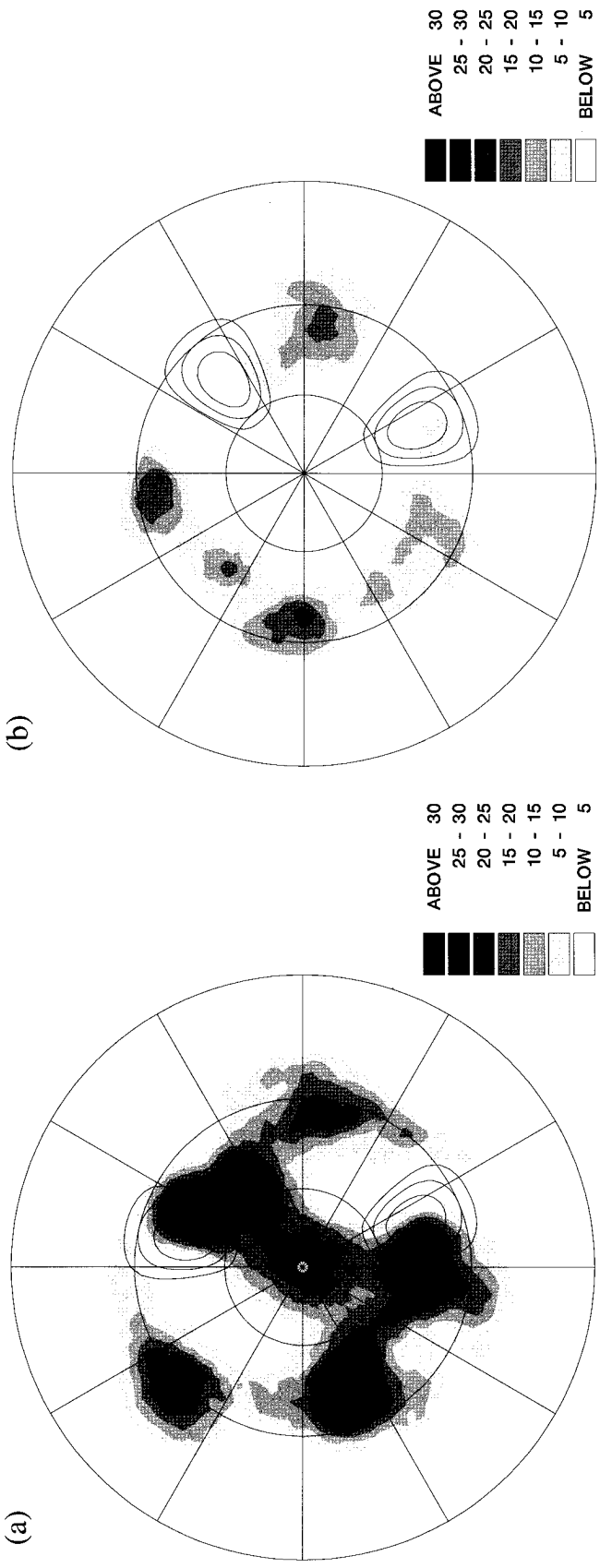

FIG. 6. The same as Fig. 5 but in experiments with a second mountain placed (a) at two wavelengths downstream of the observed single-mountain response so that the forcings by the two mountains are in phase, and (b) at one and a half wavelengths downstream of the observed single-mountain response so that the forcings by the two mountains are out of phase.

proposed by CDV must still be considered as viable candidates for explaining the persistent states of the atmosphere.

Acknowledgments. This work was supported by the Swedish National Research Council (NFR) and Nordic Council of Ministers Research (NMR) grants. We would also like to thank J. D. Opsteegh and some of the anonymous reviewers for their comments and suggestions.

APPENDIX

The Spectral Form of the Spherical Quasigeostrophic Model

Here we present the detailed derivation of the spectral form of the two-layer quasigeostrophic model (1)–(4). Assume that the dependent variables in the system, that is, ψ, τ, θ, or χ, can be written in terms of a truncated series of spherical harmonics given by

$$X(t, \lambda, \mu) = \sum_{n=m}^{N} \sum_{m=-M}^{M} X_{n,m}(t) \mathrm{P}_n^m(\mu) e^{im\lambda}. \quad \text{(A1)}$$

Here $X_{m,n}$ are the corresponding time-dependent spectral coefficients, $P_n^m(\mu)$ are normalized associated Legendre polynomials

$$\frac{1}{2} \int_{-1}^{1} [\mathrm{P}_n^m(\mu)]^2 \, d\mu = 1$$

m is the zonal wavenumber, n is the total wavenumber, and M, N are the number of retained waves. Since the spherical harmonics are orthogonal eigenfunctions of the Laplace operator, we have

$$\nabla^2 X(t, \lambda, \mu) = \sum_{n=m}^{N} \sum_{m=-M}^{M} a_0^{-2} n(n+1) X_{n,m}(t) \mathrm{P}_n^m(\mu) e^{im\lambda}. \quad \text{(A2)}$$

The Legendre polynomials $\mathrm{P}_n^m(\mu)$ have the following recursion relations for $n \geq m$, $n > 1$:

$$(\mu^2 - 1)\frac{d}{d\mu}\mathrm{P}_n^m = \sqrt{\frac{(2n+1)([n+1]^2 - m^2)}{2n+3}}\mathrm{P}_{n+1}^m - (n+1)\mu \mathrm{P}_n^m \quad \text{(A3a)}$$

$$(2n+1)\mu \mathrm{P}_n^m = \sqrt{\frac{(2n+1)([n+1]^2 - m^2)}{2n+3}}\mathrm{P}_{n+1}^m + \sqrt{\frac{(2n+1)(n^2 - m^2)}{2n-1}}\mathrm{P}_{n-1}^m. \quad \text{(A3b)}$$

The terms concerning the curvature on the right-hand side of Eqs. (3), (4) is given by

$$\boldsymbol{\nabla}(f\boldsymbol{\nabla}\tau) = f\nabla^2\tau + 2(1 - \mu^2)\frac{\partial}{\partial\mu}\tau \quad \text{(A4a)}$$

and

$$\boldsymbol{\nabla}(f\boldsymbol{\nabla}\tau) = f\nabla^2\chi + 2(1 - \mu^2)\frac{\partial}{\partial\mu}\chi. \quad \text{(A4b)}$$

Substituting (A1) and applying (A2) and (A3) to rewrite (A4) in terms of component (m, n) leads to the following:

$$\boldsymbol{\nabla}(f\boldsymbol{\nabla}\tau) = -b_0 c_p \sum_{n=m}^{N} \sum_{m=-M}^{M} [n(n+1)c_1^{mn}\tau_{m,n-1} + n(n+1)c_2^{mn}\tau_{m,n+1}]\mathrm{P}_n^m e^{im\lambda}, \quad \text{(A5a)}$$

$$\boldsymbol{\nabla}(f\boldsymbol{\nabla}\chi) = -b_0 c_p \sum_{n=m}^{N} \sum_{m=-M}^{M} [n(n+1)c_1^{mn}\chi_{m,n-1} + n(n+1)c_2^{mn}\chi_{m,n+1}]\mathrm{P}_n^m e^{im\lambda}, \quad \text{(A5b)}$$

where c_1^{mn}, c_2^{mn} are coefficients determined by the wavenumber m and n and other model parameters:

$$c_1^{mn} = \frac{2\Omega^2}{b_0 c_p}\frac{n-1}{n}\sqrt{\frac{n^2 - m^2}{4n^2 - 1}}, \quad \text{(A6a)}$$

$$c_2^{mn} = \frac{2\Omega^2}{b_0 c_p}\frac{n+2}{n+1}\sqrt{\frac{(n+1)^2 - m^2}{4(n+1)^2 - 1}}, \quad \text{(A6b)}$$

and $c_1^{mn} = 0$ for $n = 0, 1$; $c_2^{mn} = 0$ for $n = 0$.

Substituting identities (A1)–(A3) and (A5) into Eqs. (1)–(4) and then projecting onto component (m, n), one gets

$$\frac{\partial}{\partial t}\theta_{m,n} = -\mathrm{J}_{m,n}(\psi, \theta) - \sigma a_0^{-2} n(n+1)\chi_{m,n} + \delta(\theta^*_{m,n} - \theta_{m,n}) \quad \text{(A7)}$$

$$-a_0^{-2} n(n+1)\frac{\partial}{\partial t}\psi_{m,n} = -\mathrm{J}_{m,n}(\psi, \nabla^2\psi + f + f_0 h/H) - \mathrm{J}_{m,n}(\tau, \nabla^2\tau - f_0 h/H) + \frac{1}{2}a_0^{-2} n(n+1)\varepsilon_d \nabla^2(\psi_{m,n} - \tau_{m,n}) \quad \text{(A8)}$$

$$-a_0^{-2} n(n+1)\frac{\partial}{\partial t}\tau_{m,n} = -\mathrm{J}_{m,n}(\psi, \nabla^2\tau - f_0 h/H) - \mathrm{J}_{m,n}(\tau, \nabla^2\psi + f + f_0 h/H) - \frac{1}{2}a_0^{-2} n(n+1)\varepsilon_d(\psi_{m,n} - \tau_{m,n}) - b_0 c_p[n(n+1)c_1^{mn}\chi_{m,n-1} + n(n+1)c_2^{mn}\chi_{m,n+1}] + 2a_0^{-2} n(n+1)\varepsilon_i \tau_{m,n}, \quad \text{(A9)}$$

$$\theta_{m,n} = c_1^{mn}\tau_{mn-1} + c_2^{mn}\tau_{m,n+1}, \tag{A10}$$

where Jm,n is the projection of the Jacobian on component (m, n). Substituting Eq. (A10) into the left-hand side of Eq. (A7), one gets a diagnostic relation for the velocity potential χ:

$$\chi_{m,n} = \frac{a_0^2}{\sigma n(n+1)}[c_1^{mn}\tau_{m,n-1} + c_s^{mn}\tau_{m,n+1} + \mathrm{J}_{m,n}(\psi, \theta) - \delta(\theta^*_{m,n} - \theta_{m,n})]. \tag{A11}$$

Finally, using (A9) and (A11) to eliminate the velocity potential χ, one gets the following:

$$\begin{aligned} -a_1^{mn}\frac{\partial}{\partial t}\tau_{m,n-2} - a_2^{mn}\frac{\partial}{\partial t}\tau_{m,n} - a_3^{mn}\frac{\partial}{\partial t}\tau_{m,n+2} &= -\mathrm{J}_{m,n}(\psi, \nabla^2\tau - f_0 h/H) \\ &\quad - \mathrm{J}_{m,n}(\tau, \nabla^2\psi + f + f_0 h/H) \\ &\quad + b_1^{mn}[\mathrm{J}_{m,n-1}(\psi, \theta) - \delta(\theta^*_{m,n-1} - \theta_{m,n-1})] \\ &\quad + b_2^{mn}[\mathrm{J}_{m,n+1}(\psi, \theta) - \delta(\theta^*_{m,n+1} - \theta_{m,n+1})] \\ &\quad + 2a_0^{-2}n(n+1)\varepsilon_i\tau_{m,n} \\ &\quad - \frac{1}{2}a_0^{-2}n(n+1)\varepsilon_a(\psi_{m,n} - \tau_{m,n}), \end{aligned} \tag{A12}$$

where, a_j^{mn}, b_j^{mn} are coefficients determined by wavenumber m and n and other model parameters:

$$a_1^{mn} = \frac{4\Omega^2}{a_0^2 b_0 c_p \sigma}\frac{(n+1)(n-2)}{n(n-1)(2n-1)}\sqrt{\frac{(n-m^2)((n-1)^2-m^2)}{(2n+1)(2n-3)}}, \tag{A13a}$$

$$a_2^{mn} = \frac{n(n+1)}{a_0^2} + \frac{4\Omega^2}{a_0^2 b_0 c_p \sigma}\left[\frac{(n+1)^2(n^2-m^2)}{n^2(4n+1)^2} + \frac{n^2((n+1)^2-m^2)}{(n+1)^2(4(n+1)^2-1)}\right], \tag{A13b}$$

$$a_3^{mn} = \frac{4\Omega^2 n(n+3)}{a_0^2 b_0 c_p \sigma(n+1)(n+2)(2n+3)}\sqrt{\frac{((n+2)^2-m^2)((n+1)^2-m^2)}{(2n+1)(2n+5)}}, \tag{A13c}$$

$$b_1^{mn} = \frac{2\Omega^2}{\sigma}\frac{n+1}{n}\sqrt{\frac{n^2-m^2}{4n^2-1}}, \tag{A13d}$$

$$b_2^{mn} = \frac{2\Omega^2}{\sigma}\frac{n}{n+1}\sqrt{\frac{(n+1)^2-m^2}{4(n+1)^2-1}}, \tag{A13e}$$

where $a_1^{mn} = b_1^{mn} = 0$ for $n = 0, 1$; $a_3^{mn} = b_2^{mn} = 0$ for $n = 0$. Equations (A8), (A10), and (A12) describe the spectral form of the two-layer quasigeostrophic model on the sphere.

REFERENCES

Blackmon, M., 1976: A climatological spectral study of the 500 mb geopotential height of the Northern Hemisphere. *J. Atmos. Sci.,* **33,** 1607–1623.

——, S. Mullen, and G. Bates, 1986: The climatology of blocking events in a perpetual January simulation of a spectral general circulation model. *J. Atmos. Sci.,* **43,** 1379–1405.

Branstator, G., 1983: Horizontal energy propagation in a barotropic atmosphere with meridional and zonal structure. *J. Atmos. Sci.,* **40,** 1689–1708.

Charney, J., and J. DeVore, 1979: Multiple flow equilibria in the atmosphere and blocking. *J. Atmos. Sci.,* **36,** 1205–1216.

——, and D. Straus, 1980: Form-drag instability, multiple equilibria, and propagating planetary waves in baroclinic, orographically forced, planetary wave systems. *J. Atmos. Sci.,* **37,** 1157–1176.

Dole, R. M., 1986: The life cycles of persistent anomalies and blocking over the North Pacific. *Advances in in Geophysics,* Vol. 29, Academic Press, 31–69.

——, and N. Gordon, 1983: Persistent anomalies of the extratropical Northern Hemisphere wintertime circulation: Geographical distribution and regional persistence characteristics. *Mon. Wea. Rev.,* **111,** 1567–1586.

Grose, W. L., and B. Hoskins, 1979: On the influence of orography on large-scale atmospheric flow. *J. Atmos. Sci.,* **36,** 223–234.

Held, I., 1983: Stationary and quasi-stationary eddies in the extratropical troposphere: Theory. *Large-Scale Dynamical Processes in the Atmosphere,* B. Hoskins and R. Pearce, Eds., Academic Press, 127–168.

Hendon, H., 1986: Time-mean flow and variability in a nonlinear model of the atmosphere with orographic forcing. *J. Atmos. Sci.,* **43,** 433–448.

Hoskins, B., and D. Karoly, 1981: The steady linear response of a spherical atmosphere to thermal and orographic forcing. *J. Atmos. Sci.,* **38,** 1179–1196.

——, and T. Ambrizzi, 1993: Rossby wave propagation on a realistic longitudinally varying flow. *J. Atmos. Sci.,* **50,** 1651–1671.

Källén, E., 1981: The nonlinear effects of orographic and momentum forcing in a low-order, barotropic model. *J. Atmos Sci.,* **38,** 2150–2163.

——, 1985: On hysteresis-like effects in orographically forced models. *Tellus,* **37A,** 249–257.

Lau, N.-C., 1981: A diagnostic study of recurrent meteorological anomalies appearing in a 15-year simulation with a GFDL general circulation model. *Mon. Wea. Rev.,* **109,** 2287–2311.

Lorenz, E. N., 1960: Energy and numerical weather prediction. *Tellus,* **12,** 364–373.

Mak, M., 1991: Influences of the earth's sphericity in the quasi-geostrophic theory. *J. Meteor. Soc. Japan,* **69,** 497–510.

Marshall, J., and F. Molteni, 1993: Toward a dynamical understanding of planetary-scale flow regimes. *J. Atmos. Sci.,* **50,** 1792–1818.

Mo, K., and M. Ghil, 1988: Cluster analysis of multiple planetary flow regimes. *J. Geophys. Res.,* **93D,** 10 927–10 952.

O'Brien, E., and L. Branscombe, 1989: Minimal modelling of the extratropical global circulation. *Tellus,* **41A,** 292–307.

Pedlosky, J., 1981: Resonant topographic waves in barotropic and baroclinic flows. *J. Atmos. Sci.,* **38,** 2626–2641.

Plumb, R., 1985: On the three-dimensional propagation of stationary waves. *J. Atmos. Sci.,* **42,** 217–229.

Reinhold, B., 1987: Weather regimes: The challenge of extended range forecasting. *Science,* **235,** 437–441.

——, and R. Pierrehumbert, 1982: Dynamics of weather regimes: Quasi-stationary waves and blocking. *Mon. Wea. Rev.,* **110,** 1105–1145.

Roads, J., 1980a: Stable near resonant states forced by perturbation heating in a simple baroclinic model. *J. Atmos. Sci.,* **37,** 1958–1967.

——, 1980b: Stable near resonant states forced by orography in a simple baroclinic model. *J. Atmos. Sci.,* **37,** 2381–2395.

Shutts, G., 1983: The propagation of eddies in diffluent jetstreams: Eddy vorticity forcing of 'blocking' flow fields. *Quart. J. Roy. Meteor. Soc.,* **109,** 737–761.

Vautard, R., and B. Legras, 1988: On the source of midlatitude low-frequency variance. Part II: Nonlinear equilibration of weather regimes. *J. Atmos. Sci.,* **45,** 2845–2867.

Wallace, J., and D. Gutzler, 1981: Teleconnections in the geopotential height field in the Northern Hemisphere winter. *Mon. Wea. Rev.,* **109,** 784–812.

Yang, S., and B. Reinhold, 1991: How does the low-frequency variance vary? *Mon. Wea. Rev.,* **119,** 119–127.